

E14-2002-198

D. P. Kozlenko, B. N. Savenko, L. Ehm¹, K. Knorr¹,
S. Hull², V. V. Shchennikov³, V. I. Voronin³

A STRUCTURAL STUDY OF THE PSEUDO-BINARY
MERCURY CHALCOGENIDE ALLOY
HgSe_{0.7}S_{0.3} AT HIGH PRESSURE

Submitted to «Journal of Physics: Condensed Matter»

¹Institut für Geowissenschaften, Mineralogie/Kristallographie,
Universität Kiel, Olshausenstr. 40, D-24098 Kiel, Germany

²ISIS Facility, RAL, Chilton, Didcot, OX11 0QX, Oxon,
United Kingdom

³Institute for Metal Physics, Ural Branch of RAS, 620619 Ekaterinburg,
Russia

I. INTRODUCTION

II-VI pseudo-binary solid solutions of the $AB_{1-x}C_x$ type ($A = \text{Hg, Cd, Zn}$; $B, C = \text{Se, S, Te}$) have important applications in heterojunctions and opto-electronic devices.¹ The knowledge of the structural, transport and thermodynamic properties of these alloys is important for both manufacturing technology and search for additional potential applications.

It has recently been found that pseudo-binary mercury chalcogenide alloys $\text{HgSe}_{1-x}\text{S}_x$ exhibit an electronic semimetal to semiconductor phase transition under high pressure and that the transition pressure strongly depends on the sulfur content x .²⁻⁴ In a subsequent structural study it has been established that $\text{HgSe}_{1-x}\text{S}_x$ alloys with $0.3 < x < 0.6$ crystallize in the cubic zinc blende structure (space group $F\bar{4}3m$, $Z = 4$) at ambient conditions and the previously observed electronic phase transition corresponds to the structural transformation to the hexagonal cinnabar structure at $P \sim 1 \text{ GPa}$.⁵

Cinnabar phase is the ambient pressure phase of HgS (cinnabar)⁶ and it has been found under high pressure in the dichalcogenides HgSe (Refs. 7, 8), HgTe (Refs. 9-11), CdTe (Ref. 12), ZnTe (Ref. 13) and ZnSe (Ref. 14), respectively. The role of the cinnabar phase as an intermediate structure between the fourfold coordinated zinc blende and sixfold coordinated rocksalt phases in II - VI compounds has extensively been studied both experimentally^{10,11,13-16} and theoretically¹⁷⁻²⁰ during the recent years. In the cinnabar structure (space group $P3_121$, $Z = 3$) Hg (Cd, Zn) atoms occupy sites 3(a) ($u, 0, 1/3$) and chalcogene atoms occupy sites 3(b) ($v, 0, 5/6$). Depending on the values u and v , the structure of the cinnabar phase may exhibit different atomic arrangements with coordination numbers 2+4 (HgS), 4+2 (HgTe) and 6. The latter corresponds to the rocksalt structure in its hexagonal setting, having a lattice parameters ratio $c/a = \sqrt{6}$ and $u = v = 2/3$.^{11,14}

Under high pressure a decrease of the elastic constant C_{44} and the elastic constants combination $\frac{1}{2}(C_{11}-C_{12})$ has been observed in HgSe and HgTe.^{21,22} The zinc-blende - cinnabar phase transition is assumed to be driven by the softening of a transverse acoustic (TA) phonon mode. Consequently a spontaneous strain of appropriate symmetry would be a primary order parameter for this phase transition.

The structure of the pseudo-binary mercury chalcogenide alloys $\text{HgSe}_{1-x}\text{S}_x$ has recently been studied⁵ over a limited pressure range up to 3 GPa and no information on the pressure evolution of the cinnabar phase or other possible phase transitions has been obtained.

In this work we studied the structural behavior of the pseudo-binary alloy $\text{HgSe}_{0.7}\text{S}_{0.3}$ in the extended pressure range up to 8.5 GPa. The obtained structural data were used for the discussion of the zinc blende - cinnabar phase transition in the framework of Landau theory of the phase transitions²³ and the search for a possible order parameter.

II. EXPERIMENTAL

Polycrystalline samples of $\text{HgSe}_{0.7}\text{S}_{0.3}$ were prepared by melting of high purity components HgSe, HgS (99.999 %). The chemical composition of the sample was determined by means of X-ray fluorescence analysis using a "Superprobe-JCXA-733" spectrometer. The sulfur content was determined to have a value of 0.302(1).

X-ray powder diffraction measurements were performed at pressures up to 5 GPa with a Mar-2000 image plate diffractometer (MoK_α radiation, Si-(111) monochromator, $\lambda = 0.7107$ Å) using a Merrill-Bassett type diamond-anvil cell.²⁵ The pressure transmitting medium was a 4:1 methanol - ethanol mixture and the pressure was measured using the ruby fluorescence technique.²⁶ The two-dimensional powder diffraction patterns were integrated by applying the FIT2D program²⁷ to give one dimensional conventional powder diffraction profiles.

Neutron powder diffraction experiments at pressures up to 8.5 GPa were performed at the POLARIS diffractometer²⁸ (ISIS, RAL, UK), using the Paris - Edinburgh high pressure cell.²⁹ The sample volume was $V \sim 100 \text{ mm}^3$. The scattering angle range was $2\theta = 84$ - 96° and the diffractometer resolution in this geometry is approximately $\Delta d/d \approx 0.007$. Pressure were determined using the compressibility data obtained from the X-ray diffraction measurements up to 5 GPa and their extrapolation to higher pressures. The experimental data were corrected for the effects of attenuation of the incident and scattered beams by the pressure cell components.³⁰

Due to the high absorption of X-rays and neutrons by the sample typical exposure times were 16-18 h for both, X-ray and neutron diffraction experiments.

III. RESULTS

Integrated X-ray powder diffraction patterns of $\text{HgSe}_{0.7}\text{S}_{0.3}$ obtained at three different pressures are shown in fig. 1. The pattern obtained at $P = 0$ corresponds to the cubic zinc

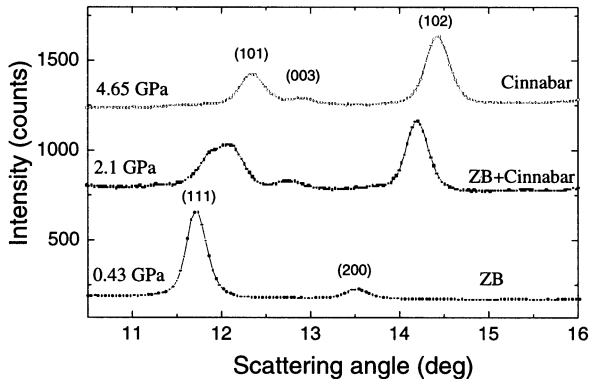


FIG. 1: Sections of integrated X-ray powder diffraction patterns of $\text{HgSe}_{0.7}\text{S}_{0.3}$ at pressures of 0.43, 2.1 and 4.65 GPa illustrating the evolution of the cinnabar phase with increasing pressure.

blende structure. Peaks steaming from the hexagonal cinnabar phase were first observed at $P = 0.97$ GPa. The contribution from the cinnabar phase increased with pressure and the single cinnabar phase was observed at pressures above 2.1 GPa.

Refinement of the diffraction data in profile matching mode using the Fullprof program³¹ provided the lattice parameters of the zinc blende and cinnabar phases as functions of pressure (table I).

The pressure dependence of the molar volume V_m (volume per molecular unit) of $\text{HgSe}_{0.7}\text{S}_{0.3}$ is shown in fig. 2. The zinc blende-cinnabar phase transition results in a volume discontinuity of $\Delta V_m/V_{m0} \approx 9\%$. There is also the relative difference between V_{m0} of the zinc blende and the cinnabar phases.

For the description of the compressibility of crystals, the 2rd order Birch-Murnaghan equation-of-state³² is commonly used

$$P = \frac{3}{2}B_0 \left(x^{-7/3} - x^{-5/3} \right) \left[1 + \frac{3}{4}(B_1 - 4)(x^{-2/3} - 1) \right], \quad (1)$$

where $x = V/V_0 = V_m/V_{m0}$ is the relative volume change, V_0 (V_{m0}) is the unit cell volume (molar volume) at $P = 0$ and B_0 and B_1 are the bulk modulus and its pressure derivative. In Eq. 1 the pressure P acts as the response variable. Since volume as well as pressure are

TABLE I: Lattice parameters of the cubic zinc blende (a_{cub}) and the hexagonal cinnabar (a , c) phases of $\text{HgSe}_{0.7}\text{S}_{0.3}$ as functions of pressure.

Pressure, GPa	a_{cub} , Å	a , Å	c , Å
0	6.024(4)	-	-
0.43(2)	6.020(4)	-	-
0.76(2)	6.008(4)	-	-
0.97(2)	5.997(4)	-	-
1.68(3)	5.975(4)	4.167(4)	9.605(4)
2.10(3)	5.945(4)	4.146(4)	9.585(4)
3.15(3)	-	4.108(4)	9.536(4)
3.78(3)	-	4.087(4)	9.524(4)
4.65(4)	-	4.066(4)	9.497(4)

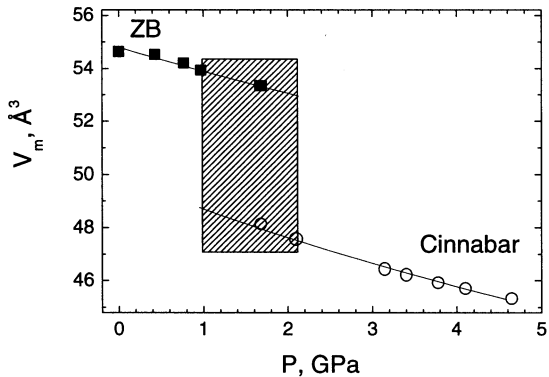


FIG. 2: The molar volume of $\text{HgSe}_{0.7}\text{S}_{0.3}$ as a function of pressure. Error bars are within the size of the symbols. The shaded area corresponds to the region of the coexistence of the zinc blende and the cinnabar phases. The solid lines represent fits of 2nd order Birch-Murnaghan equation-of-state to the experimental data.

subject to experimental error bars these errors were transformed into effective variances of the pressure $\sigma_P^{\text{eff.}}$ ³³

$$\sigma_P^{\text{eff.}} = \sqrt{\sigma_P^2 + (\sigma_V B_0/V)^2}. \quad (2)$$

These effective variances were used as weights $w = 1/(\sigma_P^{\text{eff.}})^2$ in the least squares refinement of the equation-of-state. As the bulk modulus B_0 appears in the right handed side of Eq. 2 weights were re-evaluated at each iteration step of the least squares procedure. Since the compressibility data for the zinc blende and the cinnabar phases were obtained in a rather limited pressure range, it has been found difficult to obtain B_0 and B_1 simultaneously. Hence, values of B_0 and V_{m0} at $P = 0$ for the zinc blende and the cinnabar phases were obtained from the fit of the experimental data by a 2nd order Birch-Murnaghan equation-of-state with $B_1 = 4$ (table II).

The calculated values of B_0 are higher than corresponding values obtained for the binary compounds HgSe and HgS (table II). One would expect the increase of the bulk modulus for the zinc blende phase of $\text{HgSe}_{1-x}\text{S}_x$ alloys in comparison with HgSe since partial substitution of Se atoms by S atoms decrease the average ionic radius of $X = \text{Se/S}$ anion. It is more difficult to compare values of B_0 for the cinnabar phases of $\text{HgSe}_{1-x}\text{S}_x$ and HgS, since they exist in the different pressure range. However, large difference between B_0 for $\text{HgSe}_{1-x}\text{S}_x$ and HgS may be connected with the large value of $B_1 = 11.1$ used for a description of the compressibility data in.⁹ It is well known that B_0 and B_1 are correlated parameters. Therefore it is not surprising to find smaller values for B_0 if B_1 is larger than 4 and vice versa. A similar situation was found for another mercury chalcogenide - HgTe.¹⁰ For the cinnabar phase of this compound the values $B_0 = 41(10)$ GPa and $B_1 = 3.3(2)$ were obtained while in earlier work much smaller value $B_0 = 16$ GPa was obtained with $B_1 = 7.3$.

In addition, also the pressure dependence of the lattice parameters for the cinnabar phase has been analyzed. The volume in Eq. 1 was substituted by the cube of the lattice parameters and fitted applying the 2nd order Birch-Murnaghan equation-of-state. The zero pressure compressibility $k_{a,c}$ is then given by $1/(3B_0)$. The compressibility along the a -axis is $k_a = 0.0117$ GPa⁻¹ and $k_c = 0.0045$ GPa⁻¹ along the c -axis. Hence, the compressibility in the cinnabar phase is anisotropic with $k_a \approx 2.6k_c$.

It was not possible to obtain atomic positional parameters for the cinnabar phase of $\text{HgSe}_{0.7}\text{S}_{0.3}$ from the X-ray diffraction data due to the peak overlap between the reflections of the sample and the gasket, the strong absorption by the sample and the restricted Q -

TABLE II: The bulk modulus and molar volume at ambient pressure for the zinc blende and cinnabar phases of $\text{HgSe}_{0.7}\text{S}_{0.3}$, HgSe and HgS .

	Zinc Blende		Cinnabar	
	$\text{HgSe}_{0.7}\text{S}_{0.3}$	HgSe (Ref. 21)	$\text{HgSe}_{0.7}\text{S}_{0.3}$	HgS (Ref. 9)
B_0 , GPa	58(7)	51.6(2)	39(2)	19.4(5)
B_1 , GPa	4	2.60(6)	4	11.1
V_{m0} , \AA^3	54.8(1)	56.3 (Ref. 17)	49.9(2)	47.2

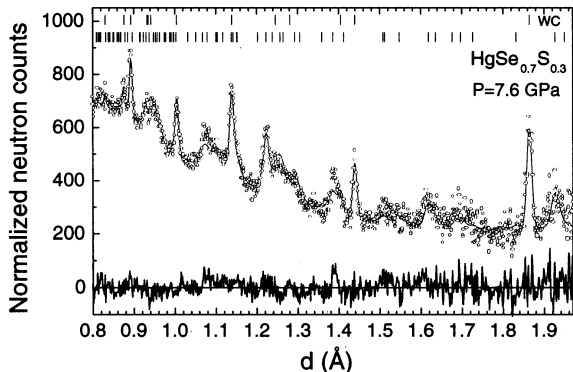


FIG. 3: The neutron diffraction pattern of the cinnabar phase of $\text{HgSe}_{0.7}\text{S}_{0.3}$ measured at the POLARIS diffractometer at $P = 7.6$ GPa and processed by the Rietveld method. Experimental points, calculated profile and difference curve (below) are shown. The contribution from the tungsten carbide (WC) anvils of the high pressure cell was also included in the calculations.

range in the X-ray experiment. However, this information could be obtained from the neutron diffraction experiments. The neutron diffraction pattern of the cinnabar phase of $\text{HgSe}_{0.7}\text{S}_{0.3}$ measured at the POLARIS diffractometer at $P = 7.6$ GPa is shown in fig. 3.

The diffraction data were refined by the Rietveld method using the program MRUA.³⁴ In the refinement procedure the structural model¹¹ in space group $P3_121$ was used, with Hg atoms occupying $3(a)$ sites ($u, 0, 1/3$) and X atoms ($X = \text{Se}, \text{S}$) occupying $3(b)$ sites ($v, 0, 5/6$), as found for the binary compounds HgX . The contribution to the diffraction pattern

TABLE III: Refined structural parameters of the cinnabar phase of $\text{HgSe}_{0.7}\text{S}_{0.3}$ at different pressures. Lattice parameters (a , c); positional parameters of Hg and $X = \text{Se/S}$ atoms (u , v) and the nearest-neighbor distances ($Hg1 - X$, $Hg2 - X$, $Hg3 - X$) are presented. The corresponding values for the binary compounds HgSe and HgS are given for comparison.

	$\text{HgSe}_{0.7}\text{S}_{0.3}$			HgSe ⁸	HgS ¹¹
P , GPa	2.7(3)	7.6(5)	8.5(6)	2.25	0
a , Å	4.127(5)	3.982(5)	3.957(5)	4.174(1)	4.14
c , Å	9.551(9)	9.389(8)	9.333(8)	9.626(1)	9.49
u	0.672(7)	0.676(7)	0.679(7)	0.666(1)	0.720(3)
v	0.529(5)	0.558(5)	0.572(5)	0.540(1)	0.480(10)
$Hg1 - X$, Å	2.49(2)	2.49(2)	2.50(2)	2.541(4)	2.36(5)
$Hg2 - X$, Å	2.93(2)	2.84(2)	2.82(2)	2.941(4)	3.10(5)
$Hg3 - X$, Å	3.28(2)	3.08(2)	3.01(2)	3.299(5)	3.30(5)
R_p , %	10.7	10.6	9.0		
R_{wp} , %	9.0	10.7	8.2		

from the tungsten carbide anvils of the high pressure cell was treated as a second phase. The lattice parameters and atomic positional parameters for the cinnabar phase of $\text{HgSe}_{0.7}\text{S}_{0.3}$ as well as the calculated nearest-neighbour interatomic distances and the obtained R -factors values at different pressures are given in table III along with the corresponding values for the binary compounds HgSe and HgS. No further phase transitions were observed in the investigated pressure range up to 8.5 GPa.

IV. DISCUSSION

The cinnabar structure is intermediate between the fourfold coordinated zinc blende and the sixfold coordinated NaCl-type structure¹⁵. The zinc blende phase of $\text{HgSe}_{0.7}\text{S}_{0.3}$ may be described in a hexagonal setting (fig. 4) using space group $P3_1$ with Hg and $X = \text{Se/S}$ atoms occupying sites $3(a)$ (x , y , z) (table IV). Hence, the zinc blende to cinnabar phase transition can be considered as a change from space group $P3_1$ to space group $P3_121$.

Its characteristic feature is a displacement of the X atoms from their initial positions

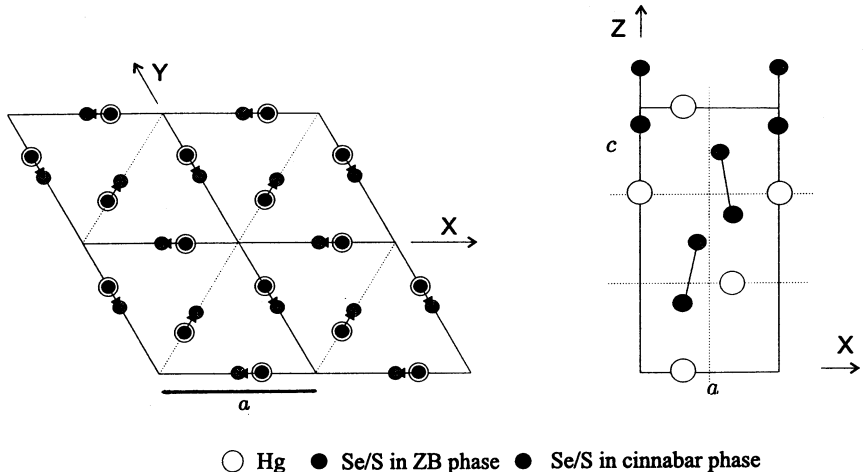


FIG. 4: Relationship between the zinc blende structure in the hexagonal setting and the cinnabar structure. Projections of the two structures on the XY plane (left) and on the XZ plane (right) are shown. Displacements of the atoms due to the transition are indicated by arrows.

TABLE IV: Atomic coordinates of the zinc blende structure described in the hexagonal setting and the cinnabar structure (values of positional parameters obtained at $P = 8.5$ GPa are given).

$X = \text{Se/S atoms}$		Hg atoms	
Zinc Blende - $3(a)$ sites	Cinnabar - $3(b)$ sites	Zinc Blende - $3(a)$ sites	Cinnabar - $3(b)$ sites
$(2/3, 0, 7/12)$	$(0.57, 0, 5/6)$	$(2/3, 0, 1/3)$	$(\approx 2/3, 0, 1/3)$
$(0, 2/3, 11/12)$	$(0.57, 0, 1/6)$	$(0, 2/3, 2/3)$	$(0, \approx 2/3, 2/3)$
$(1/3, 1/3, 1/4)$	$(0.43, 0.43, 1/2)$	$(1/3, 1/3, 0)$	$(\approx 1/3, 1/3, 0)$

$3(a)$ in space group $P3_1$ along the z - direction by $1/4 c$ and along the x and y - directions by $\varepsilon \sim 0.1 a$ to the positions $3(b)$ of the space group $P3_121$. The Hg atoms remain at nearly the same positions $3(a)$ in both phases (tables III, IV, fig. 4).

The zinc blende to cinnabar transition is a first-order phase transition. The geometry of the displacements of the X atoms due to the zinc blende - cinnabar phase transition allows us to assume that a spontaneous strain $e_4 = e_{yz} + e_{zy}$ (or $e_5 = e_{xz} + e_{zx}$, which equals e_4 for hexagonal symmetry) could be a possible order parameter.^{24,35}

We can estimate the contributions to e_4 as $e_{yz} = (a_0 - a)/c_0$ and $e_{zy} = (c_0 - c)/a_0$, where a_0 and c_0 are the lattice parameters values of the zinc blende phase in the hexagonal setting at the transition pressure and a and c are the lattice parameters of the cinnabar phase. In terms of the Landau theory of the phase transitions^{23,24}, the free energy of the system may be expanded as a function of the order parameter Q as

$$G = \frac{1}{2}a_2(P - P_c)Q^2 + \frac{1}{4}a_4Q^4 + \frac{1}{6}Q^6. \quad (3)$$

In the case of first-order phase transitions, the order parameter Q undergoes a jump at a transition point and the value P_c in Eq. 3 does not correspond to the transition pressure and determines only the point where a coefficient at the quadratic term of free energy expansion changes its sign. Assuming $Q = e_4$ one obtains the evolution of the order parameter in the cinnabar phase expressed as^{23,24}

$$e_4^2 = \frac{2}{3}e_{40}^2 \left\{ 1 + \left[1 - \frac{3}{4} \left(\frac{P - P_c}{P_{tr} - P_c} \right) \right]^{1/2} \right\}. \quad (4)$$

Here P_{tr} is the transition pressure, and the jump in e_4 at P_{tr} is given by

$$e_{40}^2 = \frac{4a_2}{a_4}(P_{tr} - P_c). \quad (5)$$

The experimental $e_4^2(P)$ data fitted by Eq. 4 are shown in fig. 5. The experiment and calculation are in good agreement, and the following values of parameters were obtained: $e_{40} = 0.030(1)$, $P_c = 2.25(8)$ GPa. Values of $a_0 = 4.24$ Å and $c_0 = 10.387$ Å were obtained from the cubic lattice parameter of the zinc blende phase (table I) at $P_{tr} = 0.97$ GPa, which was used as the transition pressure.

Assuming the spontaneous strain e_{44} to be a primary order parameter for the zinc blende - cinnabar phase transition, a softening of the elastic constant C_{44} in the vicinity of the transition point should be expected.³⁶ In the high-pressure studies of the elastic constants of HgSe²¹ and HgTe²² a decrease of the C_{44} has been observed on approaching the zinc blende - cinnabar transition pressure. This is in agreement with our considerations.

The cinnabar structure is closely related to the cubic NaCl-type structure.¹⁵ The NaCl-type structure in its hexagonal setting may be described using the same space group as for the cinnabar structure, $P3_121$, with atomic positional parameters $u = v = 2/3$. As it follows from table III, with increasing pressure the positional parameter of the Hg atoms varies slowly and remains close to its value in the zinc blende structure or the corresponding

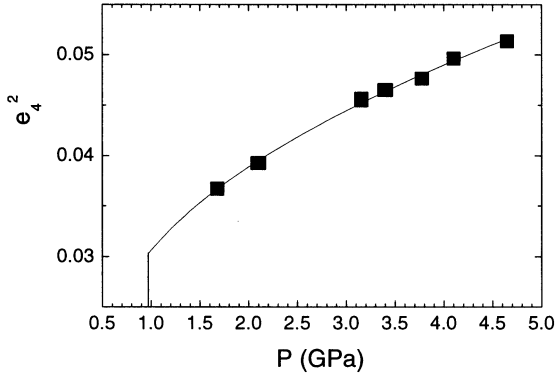


FIG. 5: Square of the spontaneous strain e_4 as a function of pressure. The solid line is the fit to the experimental data using Eq. 4. Error bars are within the symbols size.

value for the NaCl-type structure, $u \sim 0.67$. The positional parameter of the $X = \text{Se/S}$ atoms which shifts from $v = 0.67$ to $v \sim 0.53$ at the phase transition, increases up to 0.57 in the pressure range 2.7 - 8.5 GPa starting to approach the value corresponding to the NaCl-type cubic structure.

There are three pairs of nearest-neighbor distances between $X = \text{Se/S}$ and Hg atoms ($Hg1 - X$, $Hg2 - X$ and $Hg3 - X$) with rather close values in the cinnabar structure.¹¹ In $\text{HgSe}_{0.7}\text{S}_{0.3}$ the pressure increase from 2.7 to 8.5 GPa causes the shortest $Hg1 - X$ distance to remain almost constant whilst the two other distances decrease approaching the value of the first one (fig. 6, table III). This corresponds to an increasing of $X - Hg - X$ angle (from 168.1° to 173.8°) and a decrease in the $Hg - X - Hg$ angle from 105.4° to 99.0° . Thus, the cinnabar structure of $\text{HgSe}_{0.7}\text{S}_{0.3}$ approaches the NaCl-type cubic structure with increasing pressure, where the distances $Hg1 - X = Hg2 - X = Hg3 - X$ and the interatomic $X - Hg - X$ and $Hg - X - Hg$ angles have values of 180° and 90° , respectively.

A description of the coordination of the cinnabar phase of $\text{HgSe}_{0.7}\text{S}_{0.3}$ may be performed using the following ratio: $r = (l_{Hg2-X} - l_{Hg1-X}) / (l_{Hg3-X} - l_{Hg2-X})$. Values of $r < 1$ correspond to a 4+2 coordination, $r > 1$ to a 2+4 coordination and $r = 1$ to the sixfold

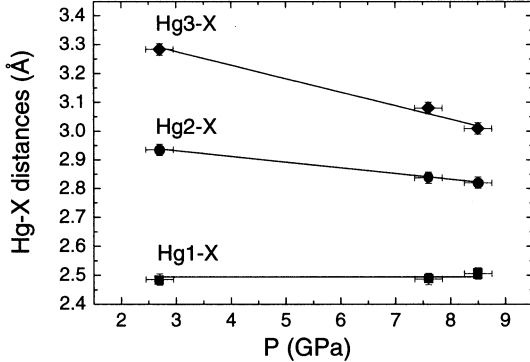


FIG. 6: The nearest-neighbor distances between Hg and $X = \text{Se/S}$ atoms in $\text{HgSe}_{0.7}\text{S}_{0.3}$ as functions of pressure. The solid lines are linear interpolations of the experimental data.

coordination. The calculated value r for $\text{HgSe}_{0.7}\text{S}_{0.3}$ varies from 1.26 to 1.68 with the pressure increasing from 2.7 to 8.5 GPa. The increase of the distortion index r shows that the difference between the $Hg3 - X$ and $Hg2 - X$ distances decreases faster than the difference between distances $Hg2 - X$ and $Hg1 - X$ on pressure increase. The comparison between $\text{HgSe}_{0.7}\text{S}_{0.3}$ and the parent binary compounds HgSe and HgS shows that the cinnabar structure of $\text{HgSe}_{0.7}\text{S}_{0.3}$ is similar to that of HgSe ($r = 1.1$, calculated from data reported in⁸) and less distorted with respect to the NaCl - type cubic structure ($r = 1$) than the cinnabar structure of HgS ($r = 3.7$).¹¹ This means that the phase transition between the cinnabar and NaCl-type phases in $\text{HgSe}_{0.7}\text{S}_{0.3}$ might be expected to occur at nearly the same pressure as for HgSe, $P \sim 16$ GPa. In³⁸ a decrease of the electrical resistivity by several orders of magnitude was observed in $\text{HgSe}_{0.7}\text{S}_{0.3}$ at $P \sim 15$ GPa. Such a behavior corresponds to an electronic semiconductor-metal phase transition which accompanies the structural phase transition from the cinnabar to the NaCl-type structure in binary mercury chalcogenides HgSe, HgTe.^{10,37}

V. CONCLUSIONS

In the present work the structure of the pseudo-binary mercury chalcogenide alloy $\text{HgSe}_{0.7}\text{S}_{0.3}$ was studied in the pressure range up to 8.5 GPa by means of X-ray and neutron powder diffraction. At the pressure $P=0.97$ GPa a phase transition from the cubic zinc blende to the hexagonal cinnabar structure was observed in agreement with previous studies. Both phases coexist in the vicinity of the transition pressure. The coordination and geometrical features of the cinnabar phase of $\text{HgSe}_{0.7}\text{S}_{0.3}$ are similar to those of HgSe.

The obtained structural parameters were used for the analysis of the geometrical relationship between the zinc blende and cinnabar phases. It was found that the possible order parameter for the zinc blende - cinnabar structural transformation is the spontaneous strain e_4 (or e_5). This conclusion is supported by a softening of the elastic constant C_{44} at this phase transition as observed in HgSe^{21} and HgTe^{22} . Hence the proposed model of the zinc blende - cinnabar phase transition may be generalized for the case of other mercury chalcogenides exhibiting this phase transition - HgSe, HgTe, CdTe, ZnTe and their pseudo-binary solutions.

With increasing pressure the interatomic angles and distances of the cinnabar structure approach the values corresponding to the NaCl-type cubic structure. This let us expect a phase transition from the hexagonal cinnabar structure to the cubic NaCl-type structure at higher pressure.

Acknowledgments

The work was supported by the Russian Foundation for Basic Research, grants 00-02-17199 and 01-02-17203.

References

- ¹ P. Letardi, N. Motta, and A. Balzarotti, J. Phys. C: Solid State Phys. **20**, 2853 (1987).
- ² V.V. Shchennikov, N.P. Gavaleshko, V.M. Frasunyak, and V.I. Osotov, Phys. Solid State **37**, 1311 (1995).
- ³ V.V. Shchennikov, A.E. Kar'kin, N.P. Gavaleshko, and V.M. Frasunyak, Phys. Solid State **39**, 1528 (1997).

- ⁴ V.V. Shchennikov. In: "Process, equipment and materials control in integrated circuit manufacturing IV", ed. by A.J.Toprac and Kim Dang, Proceedings of SPIE, **3507**, 254 (1998).
- ⁵ V.I. Voronin, V.V. Shchennikov, I.F. Berger, V.P. Glazkov, D.P. Kozlenko, B.N. Savenko, and S.V. Tikhomirov, Phys. Solid State **43**, 2165 (2001).
- ⁶ K.L. Aurivillius, Acta Chem. Scand. **4**, 1423 (1950).
- ⁷ A.N. Mariano and E.P. Wareikos, Science **142**, 672 (1963).
- ⁸ M.I. McMahon, R.J. Nelmes, H. Liu, and S.A. Belmonte, Phys. Rev. Lett. **77**, 1781 (1996).
- ⁹ A. Werner, H.D. Hocheimer, K. Strössner, and A. Jayaraman, Phys. Rev. B **28**, 3330 (1983).
- ¹⁰ A. San-Miguel, N.G. Wright, M.I. McMahon, and R.J.Nelmes, Phys. Rev. B **51**, 8731 (1995).
- ¹¹ N.G. Wright, M.I. McMahon, R.J. Nelmes, and A. San-Miguel, Phys. Rev. B **48**, 13111 (1993).
- ¹² M.I. McMahon, R.J. Nelmes, N.G. Wright, and D.R. Allan, Phys. Rev. B **48**, 16246 (1993).
- ¹³ R.J. Nelmes, M.I. McMahon, N.G. Wright, and D.R.Allan, Phys. Rev. Lett., **73**, 1805 (1994).
- ¹⁴ J. Pellicer-Porres, A. Segura, V. Muñoz, J. Zúñiga, J.P. Itié, A.Polian, and P.Munsch, Phys. Rev. B **65**, 012109 (2001).
- ¹⁵ M.I. McMahon, and R.J. Nelmes, Phys. Stat. Sol. (b) **198**, 389 (1996).
- ¹⁶ A. San-Miguel, A. Polian, and J.P. Itié, J. Phys. Chem. Solids **56**, 555 (1995).
- ¹⁷ Z.W. Lu, D.Singh, and H.Krakauer, Phys. Rev. B **39**, 10154 (1989).
- ¹⁸ M. Côté, O.Zakharov, A.Rubio, and M.L.Cohen, Phys. Rev. B **55**, 13025 (1997).
- ¹⁹ A. Qteish and A.Múnoz, Phys. Status Solidi B **223**, 417 (2001).
- ²⁰ G.D. Lee and J. Ihm, Phys. Rev. B **53**, R7622 (1996).
- ²¹ P.J. Ford, A.J. Miller, G.A. Saunders, Y.K. Yoğurtçü, J.K. Furdyna, and M. Jaczynski, J. Phys. C: Solid State Phys. **15**, 657 (1982).
- ²² A.J. Miller, G.A. Saunders, Y.K. Yoğurtçü, and A.E. Abey, Phil. Mag. **43**, 1447-71 (1981).
- ²³ L.D. Landau, Phys. Z. Sov. Un., **11**, 26 (1937).
- ²⁴ A.D. Bruce and R.A.Cowley, Structural Phase Transitions (Taylor & Francis Ltd., London, 1981).
- ²⁵ L. Merrill, and W.A. Bassett, Rev. Sci. Instrum. **45**, 290 (1974).
- ²⁶ G.J. Piermarini, S. Block, J.D. Barnett, and R.A. Forman, J. Appl. Phys. **46**, 2774 (1975).
- ²⁷ A.P. Hammersley, S.O. Svensson, M. Hanfland, A.N. Fitch, and D. Häusermann, High Pressure Research **14**, 235 (1996).
- ²⁸ S. Hull, R.I. Smith, W.I.F. David, A.C. Hannon, J. Mayers, and R. Cywinski, Physica B **180-181**, 1000 (1992).

- ²⁹ J.M. Besson, R.J. Nelmes, G. Hamel, J.S. Loveday, G. Weill, and S. Hull, *Physica B* **180-181**, 907 (1992).
- ³⁰ R.M. Wilson, J.S. Loveday, R.J. Nelmes, S. Klotz, and W.G. Marshall, *Nucl. Instr. and Meth. in Phys. Res. A* **334**, 145 (1995).
- ³¹ J. Rodriguez-Carvajal, *Physica B* **55**, 192 (1993).
- ³² F. Birch, *J. Geophys. Res.* **83**, 1257 (1978).
- ³³ R.J. Angel, Equations of State, in "Reviews in Mineralogy and Geochemistry", edited by R.M. Hazen and R T Downs (Mineralogical Soc. of America, Washington D.C., 2000) Vol. **41**, High-Temperature and High-Pressure Crystal Chemistry, pp. 35-59.
- ³⁴ V.B. Zlokazov, and V.V. Chernyshev, *J. Appl. Cryst.* **25**, 447 (1992).
- ³⁵ M.A. Carpenter, and E.K.H. Salje, *Eur. J. Mineral.* **10**, 693 (1998).
- ³⁶ R.A. Cowley, *Phys. Rev. B* **13**, 4877 (1976).
- ³⁷ T.L. Huang, and A.L. Ruoff, *Phys. Rev. B* **31**, 5976 (1985).
- ³⁸ V.V. Shchennikov, N.P. Gavaleshko, and V.M. Frasunyak, *Phys. Solid State* **35**, 199 (1993).

Received on August 27, 2002.

Козленко Д. П. и др.

E14-2002-198

Исследование структуры псевдобинарного сплава халькогенидов ртути $\text{HgSe}_{0,7}\text{S}_{0,3}$ при высоких давлениях

Проведено исследование структуры псевдобинарного сплава халькогенидов ртути $\text{HgSe}_{0,7}\text{S}_{0,3}$ методами рентгеновской и нейтронной порошковой дифракции при давлениях до 8,5 ГПа. При давлении $P \sim 1$ ГПа наблюдался переход из кубической структуры типа сфалерита в гексагональную структуру типа киновари. Полученные структурные параметры использовались для анализа геометрической взаимосвязи между структурами сфалерита и киновари и рассмотрения фазового перехода сфалерит–киноварь в рамках теории фазовых переходов Ландау. Установлено, что возможным параметром порядка для этого структурного фазового перехода является спонтанная деформация e_4 . Этот результат согласуется с наблюдаемым поведением упругих модулей некоторых халькогенидов ртути в окрестности данного фазового перехода.

Работа выполнена в Лаборатории нейтронной физики им. И. М. Франка ОИЯИ.

Препринт Объединенного института ядерных исследований. Дубна, 2002

Kozlenko D. P. et al.

E14-2002-198

A Structural Study of the Pseudo-Binary Mercury Chalcogenide Alloy $\text{HgSe}_{0,7}\text{S}_{0,3}$ at High Pressure

The structure of the pseudo-binary mercury chalcogenide alloy $\text{HgSe}_{0,7}\text{S}_{0,3}$ has been studied by means of X-ray and neutron powder diffraction at pressure up to 8.5 GPa. A phase transition from the cubic zinc blende structure to the hexagonal cinnabar structure was observed at $P \sim 1$ GPa. The obtained structural parameters were used for the analysis of the geometrical relationship between the zinc blende and the cinnabar phases. The zinc blende–cinnabar phase transition is discussed in the framework of Landau theory of the phase transitions. It was found that the possible order parameter for the structural transformation is the spontaneous strain e_4 . This assignment agrees with previously observed high pressure behaviour of the elastic constants of other mercury chalcogenides.

The investigation has been performed at the Frank Laboratory of Neutron Physics, JINR.

Preprint of the Joint Institute for Nuclear Research. Dubna, 2002

Макет *Т. Е. Попеко*

Подписано в печать 01.10.2002.

Формат 60 × 90/16. Бумага офсетная. Печать офсетная.

Усл. печ. л. 1,18. Уч.-изд. л. 1,3. Тираж 300 экз. Заказ № 53534.

Издательский отдел Объединенного института ядерных исследований
141980, г. Дубна, Московская обл., ул. Жолио-Кюри, 6.